

The mechanical, thermo-physical and ultrasonic properties of scandium nitride in B1 and B2 phases

Anurag Singh^{1,2,*}, Jyoti Bala³, Shakti Pratap Singh⁴, Devraj Singh¹

¹Department of Physics, Prof. Rajendra Singh (Rajju Bhaiya) Institute of Physical Sciences for Study and Research, Veer Bahadur Singh Purvanchal University, Jaunpur 222003, India

²Department of Physics, Dr. Shyama Prasad Mukherjee Government Degree College, Bhadohi 221401, India

³Department of Physics, Goswami Ganesh Dutta Sanatan Dharma College, Sector 32, Chandigarh 160032, India

⁴Department of Physics, Government Polytechnic, Kuru, Pindra, Varanasi 221206, India

*Email: anuragrajpoot440@gmail.com

Received: 15 February 2024; Accepted for publication: 9 November 2024

Abstract. The mechanical, elastic, thermophysical and nonlinear ultrasonic effects of scandium nitride (ScN) have been interrogated in both B1 and B2 phases at 300 K. The estimation of the second- and third-order elastic constants (SOECs and TOECs) for ScN has been done by the application of Coulomb and Born-Mayer potential model. ScN is elastically stable in both phases. The mechanical properties have been determined with the help of SOECs using Voigt-Reuss-Hill approximation. The ScN has ductile nature in B1 phase whereas brittle nature in B2 phase. Further, the nonlinear ultrasonic velocities, Debye average velocities and Debye temperatures have been estimated with the calculated values of SOECs. Then, the thermophysical properties of ScN have been computed along the $\langle 100 \rangle$, $\langle 110 \rangle$ and $\langle 111 \rangle$ crystallographic orientations. Finally, the ultrasonic attenuation due to thermoelastic mechanism and phonon-phonon interaction has been figured along suitable crystallographic directions for the ScN at 300 K. The attenuation due to phonon-phonon interaction dominated over the thermal attenuation. The attained results have been compared and discussed with existing findings on the ScN in both B1 and B2 phases.

Keywords: Scandium nitride, elastic constants, thermophysical properties, ultrasonic attenuation.

Classification numbers: 2.1.3., 2.2.1., 2.5.3., 2.10.3.

1. INTRODUCTION

Recently, among group III-V based materials, scandium nitride (ScN) has received much attention because it has a wide band gap just like GaN, AlN, and InN [1 - 4]. The ScN is a

transition metal compound with peculiar properties such as larger mechanical strength, greater stability and hardness at high temperatures. It has a low lattice constant compared to GaN and can be used as a substrate for GaN-based devices [5]. Moreover, the ScN has a good thermal stability and high melting temperature in comparison to other nitrides of the same group [6]. According to Hagg's empirical prediction [7], the structure of lattices can be bcc, fcc or hcp when the ratio of metal to non-metal atom radii is greater than 1.70. Mnisi [8] investigated the structural, mechanical, electronic and optical properties of the ScN in B1, B2, B3 and B8 structures using the first principle density functional theory. In this investigation, it has been found that ScN is a semiconductor in B1 phase with a lattice parameter of 4.57 Å, while metallic in B2 phase with a lattice parameter of 2.82 Å. A systematic study of the ScN was carried out by Takeuchi on the ground state properties and stability in the B1, B2, B3, B4 and B8 structures using the first principles method [9]. The rock salt B1 structure has the ground state configuration and the calculations showed the possibility of phase transition to a metallic B2 structure at high pressure. Duman *et al.* studied the structural, electronic and dynamical properties of rock salt semiconductor GaN and ScN using ab initio method [10]. The phonon dispersion curves for these two materials have also been discussed by them. Maachou *et al.* calculated the band structure, bulk modulus, lattice parameter and cohesion energy of ScX (X = N, P, As and Sb) for the B1 and B2 structures using the first principles method [11]. They also reported the electronic band structure of ScX in B1 and B2 phases. Few more important properties of ScN were examined by Stampfl *et al.* using generalized gradient approximation (GGA) model [12]. They showed semiconducting as well as semimetallic nature of the ScN. First principle study of the B1, B2, B3, B4, Bc and A5 structured ScN at high pressure has been reported by Yagoub *et al.* [13]. Their results clearly indicated a structural transition from B1 to B2 at high pressure for the ScN. The structural, vibrational and thermophysical properties of ScN and their harmonic effects were propounded by Tahri *et al.* [14]. They found that crystal structure has a large influence on the material properties. The structural, thermodynamical and elastic behaviour of Sc_xAl_{1-x}N in B1 and B4 phases were studied by Ambacher *et al.* [15]. Particular attention has been paid to the directional anisotropy of the different crystal lattices of Sc atoms substituted on increasing number of Al atoms by them.

Although the chosen compound ScN is very important for its applications in industries, yet limited literatures are available for the ScN in B1 and B2 phases [16 - 19]. The two hexagonal and tetragonal phases of ScX have been investigated by Seksaria *et al.* [16]. They have reported that the hexagonal structure of the ScX has semiconducting nature while the tetragonal structure of the ScX has semi-metallic nature. The dynamical, electronic and thermophysical properties of the B1 structured ScN have been calculated using the first principle method to find lattice parameters by Xue *et al.* [17]. The electronic structure of transition metal doped ScN has been reported by Sukkabot [18]. The findings of this investigation have inferred that lattice parameters, volume and magnetic properties have been modified due to the presence of dopants. The structural, electronic and elastic properties including lattice parameters, elastic constants, elastic moduli and band gap have been studied by Ekuma *et al.* [19] using first principle methods. Even the published works have not elaborated the ultrasonic nonlinear properties of the ScN such as ultrasonic Grüneisen parameters and ultrasonic attenuation. This stimulated us to investigate the mechanical, thermo-physical and ultrasonic parameters of the ScN single crystal in both B1 (NaCl-type) and B2 (CsCl-type) phases along the <100>, <110> and <111> directions at room temperature. We applied Coulomb and Born-Mayer potential theoretical model and used MATLAB software to calculate elastic constants which were further used to calculate mechanical, thermophysical and ultrasonic parameters of the ScN. The theoretical results have been compared and discussed with existing literature.

2. THEORY

For computing ultrasonic attenuation, mechanical parameters and thermal properties, the second- and third-order elastic constants (SOECs and TOECs) play a critical role for the finding the materials nature as well as materials applicability of materials. The SOECs and TOECs have been computed at absolute zero (C_{IJ}^0 and C_{IJK}^0) on account of Brugger's definition of the elastic constants [20,21]. Leibfried and Haln [22], Leibfried and Ludwig [23], Ghate [24] and Hiki and Mori [25] developed a method for computation of the higher order elastic constants for the B1 and B2 structured single crystalline materials, since scandium nitride exists in both phases, i.e., B1 and B2. The interaction potential $\phi(r_{\mu\nu})$ between μ^{th} and ν^{th} ions is the sum of long-range coulomb potential $\phi_C(r_{\mu\nu})$ and short range Born Mayer repulsive potential $\phi_B(r_{\mu\nu})$. The interaction potential $\phi(r_{\mu\nu})$ can be expressed as [26]

$$\phi(r_{\mu\nu}) = \phi_C(r_{\mu\nu}) + \phi_B(r_{\mu\nu}), \quad (1)$$

$\phi_C(r_{\mu\nu})$ and $\phi_B(r_{\mu\nu})$ may be expressed as

$$\phi_C(r_{\mu\nu}) = \pm \left(\frac{e^2}{r_0} \right) \quad \text{and} \quad \phi_B(r_{\mu\nu}) = A \exp\left(-\frac{r_0}{b}\right).$$

where e signifies for electronic charge, r_0 for nearest neighbour distance and b for hardness parameter, respectively. Here \pm sign stands for cations and anions. The strength parameter A is specified by [26]

$$A = -3b \left(\frac{e^2}{r_0^2} \right) \left[6 \exp\left(-\frac{r_0}{b}\right) + 12\sqrt{2} \exp\left(-\frac{\sqrt{2}r_0}{b}\right) \right]^{-1}. \quad (2)$$

The SOECs and TOECs consist of two parts which are static part at 0 K and 'vib' part at required temperature. The elastic constants for B1 structured ScN are as follows:

$$C_{IJ} = C_{IJ}^0 + C_{IJ}^{\text{vib}} \quad \text{and} \quad C_{IJK} = C_{IJK}^0 + C_{IJK}^{\text{vib}}.$$

The static part of second and third order elastic constants for B1 phase at 0 K is expressed as

$$\begin{aligned} C_{11}^0 &= \frac{3e^2}{2r_0^4} S_5^{(2)} + \frac{1}{br_0} \left(\frac{1}{r_0} + \frac{1}{b} \right) \varphi(r_0) + \frac{2}{br_0} \left(\frac{1}{\sqrt{2}r_0} + \frac{1}{b} \right) \varphi(\sqrt{2}r_0), \\ C_{12}^0 &= C_{44}^0 = \frac{3e^2}{2r_0^4} S_5^{(1,1)} + \frac{1}{br_0} \left(\frac{1}{\sqrt{2}r_0} + \frac{1}{b} \right) \varphi(\sqrt{2}r_0), \\ C_{111}^0 &= -\frac{15e^2}{2r_0^4} S_7^{(3)} - \frac{1}{b} \left(\frac{3}{r_0^2} + \frac{3}{br_0} + \frac{1}{b^2} \right) \varphi(r_0) - \frac{1}{2b} \left(\frac{3\sqrt{2}}{r_0^2} + \frac{6}{br_0} + \frac{2\sqrt{2}}{b^2} \right) \varphi(\sqrt{2}r_0), \\ C_{112}^0 &= C_{166}^0 = -\frac{15e^2}{2r_0^4} S_7^{(2,1)} - \frac{1}{4b} \left(\frac{3\sqrt{2}}{r_0} + \frac{6}{br_0} + \frac{2\sqrt{2}}{b^2} \right) \varphi(\sqrt{2}r_0), \\ C_{123}^0 &= C_{144}^0 = C_{456}^0 = -\frac{15e^2}{2r_0^4} S_7^{(1,1,1)}. \end{aligned}$$

$$\varphi(r_0) = A \exp\left(-\frac{r_0}{b}\right) \quad \text{and} \quad \varphi(\sqrt{2}r_0) = A \exp\left(-\frac{\sqrt{2}r_0}{b}\right).$$

The values of lattice sum are

$$\begin{aligned} S_3^{(1)} &= -0.58252, \quad S_5^{(2)} = -1.04622, \quad S_3^{(1,1)} = 0.23185, \\ S_7^{(3)} &= -1.36852, \quad S_7^{(2,1)} = 0.16115, \quad S_7^{(1,1,1)} = -0.09045. \end{aligned}$$

Vibrational contributions of the SOECs and TOECs (C_{IJ}^{Vib} and C_{IJK}^{Vib}) for B1 structured ScN are given as

$$\begin{aligned} C_{11}^{Vib} &= f^{(1,1)}G_1^2 + f^{(2)}G_2, \\ C_{12}^{Vib} &= f^{(1,1)}G_1^2 + f^{(2)}G_{1,1}, \\ C_{44}^{Vib} &= f^{(2)}G_{1,1}, \\ C_{111}^{Vib} &= f^{(1,1,1)}G_1^3 + 3f^{(2,1)}G_2G_1 + f^{(3)}G_3, \\ C_{112}^{Vib} &= f^{(1,1,1)}G_1^3 + f^{(2,1)}G_1(2G_{1,1} + G_2) + f^{(3)}G_{2,1}, \\ C_{123}^{Vib} &= f^{(1,1,1)}G_1^3 + 3f^{(2,1)}G_1G_{1,1} + f^{(3)}G_{1,1,1}, \\ C_{144}^{Vib} &= f^{(2,1)}G_1G_{1,1} + f^{(3)}G_{1,1,1}, \\ C_{166}^{Vib} &= f^{(2,1)}G_1G_{1,1} + f^{(3)}G_{2,1}, \\ C_{456}^{Vib} &= f^{(3)}G_{1,1,1}. \end{aligned}$$

where, $f^{(2)} = f^{(3)} = \frac{\hbar\omega_0}{8r_0^3} \coth x$,

$$\begin{aligned} f^{(1,1)} &= f^{(2,1)} = -\frac{\hbar\omega_0}{96r_0^3} \left\{ \frac{\hbar\omega_0}{2k_B T \sinh^2 x} + \coth x \right\}, \\ f^{(1,1,1)} &= -\frac{\hbar\omega_0}{384r_0^3} \left\{ \frac{(\hbar\omega_0)^2 \coth x}{6(k_B T)^2 \sinh^2 x} + \frac{\hbar\omega_0 \coth x}{2k_B T \sinh^2 x} + \coth x \right\}. \end{aligned}$$

here $x = \frac{\hbar\omega_0}{2k_B T}$; $\hbar = \frac{h}{2\pi}$ and h is Planck's constant. Expressions of G_n are given by the following relations.

$$\begin{aligned} G_1 &= 2[(2 + 2\rho_0 - \rho_0^2)\varphi(r_0) + 2(\sqrt{2} + 2\rho_0 - \sqrt{2}\rho_0^2)\varphi(\sqrt{2}r_0)]H, \\ G_2 &= 2[(-6 - 6\rho_0 - \rho_0^2 + \rho_0^3)\varphi(r_0) + (-3\sqrt{2} - 6\rho_0 - \sqrt{2}\rho_0^2 + 2\rho_0^3)\varphi(\sqrt{2}r_0)]H, \\ G_3 &= 30 + 30\rho_0 + 9\rho_0^2 - \rho_0^3 - \rho_0^4)\varphi(r_0) + \left(\frac{15}{2}\sqrt{2} + 15\rho_0 + \frac{9}{2}\sqrt{2}\rho_0^2 - \rho_0^3 - \sqrt{2}\rho_0^4\right)\varphi(\sqrt{2}r_0)\}H, \\ G_{1,1} &= [(-3\sqrt{2} - 6\rho_0 - \sqrt{2}\rho_0^2 + 2\rho_0^3)\varphi(\sqrt{2}r_0)]H, \\ G_{2,1} &= \left[\left(\frac{15}{\sqrt{2}} + 15\rho_0 + \frac{9}{\sqrt{2}}\rho_0^2 - \rho_0^3 - \sqrt{2}\rho_0^4\right)\varphi(\sqrt{2}r_0)\right]H, \\ G_{1,1,1} &= 0. \end{aligned}$$

where H is given by the following expression

$$H = [(\rho_0 - 2)\varphi(r_0) + 2(\rho_0 - \sqrt{2})\varphi(\sqrt{2}r_0)]^{-1} \text{ and } \rho_0 = \frac{r_0}{b}.$$

The expression for the static parts of second- and third-order elastic constants for the B2 structured ScN are as follows:

$$\begin{aligned} C_{11}^0 &= \frac{3e^2}{8r_0^4} S_5^{(2)} + \frac{3\phi(r_1)}{br_0} \left(\frac{\sqrt{3}}{3r_0} + \frac{1}{b}\right) + \frac{2\phi(r_2)}{br_0} \left(\frac{1}{2r_0} + \frac{1}{b}\right), \\ C_{12}^0 &= C_{44}^0 = \frac{3e^2}{8r_0^4} S_5^{(1,1)} + \frac{\phi(r_2)}{br_0} \left(\frac{1}{2r_0} + \frac{1}{b}\right), \\ C_{111}^0 &= -\frac{15e^2}{8r_0^4} S_7^{(3)} - \frac{\phi(r_1)}{9b} \left(\frac{\sqrt{3}}{r_0^2} + \frac{3}{br_0} + \frac{\sqrt{3}}{b^2}\right) - \frac{\phi(r_2)}{2b} \left(\frac{3}{r_0^2} + \frac{6}{br_0} + \frac{4}{b^2}\right), \\ C_{112}^0 &= C_{166}^0 = -\frac{15e^2}{8r_0^4} S_7^{(2,1)} - \frac{\phi(r_1)}{9b} \left(\frac{\sqrt{3}}{r_0^2} + \frac{3}{br_0} + \frac{\sqrt{3}}{b^2}\right), \\ C_{123}^0 &= C_{456}^0 = C_{144}^0 = -\frac{15e^2}{8r_0^4} S_7^{(1,1,1)} - \frac{\phi(r_1)}{9b} \left(\frac{\sqrt{3}}{r_0^2} + \frac{3}{br_0} + \frac{\sqrt{3}}{b^2}\right). \end{aligned}$$

where $r_1 = \sqrt{3}r_0$; $r_2 = 2r_0$.

$$\phi(r_1) = A \exp\left(-\frac{r_1}{b}\right); \quad \phi(r_2) = A \exp\left(-\frac{r_2}{b}\right); \quad A = \frac{bZ_0e^2}{r_0^2} [8\sqrt{3}\exp\left(-\frac{r_1}{b}\right) + 12\exp\left(-\frac{r_2}{b}\right)].$$

The expressions for the vibrational part of elastic constants for B2 structured ScN are as follows:

$$C_{IJK\dots}^{VIB} = a_{IJK\dots} T \quad \text{where} \quad a_{IJK\dots} = L_1 k_B \left. \frac{\partial C_{IJK\dots}^S}{\partial r} \right|_{r=r_0} + \frac{F_{IJK\dots}^{VIB}}{TV_C},$$

$$L_1 = -r_0 \left[\frac{8}{3}(2\rho_1 + 2\rho_1^2 - \rho_1^3)\phi(r_1) + \frac{3}{2}(2\rho_2 + 2\rho_2^2 - \rho_2^3)\phi(r_2) \right] Y^{-1}, \quad Y = \left[\frac{8}{3}(\rho_1^2 - 2\rho_1)\phi(r_1) + \frac{3}{2}(\rho_2^2 - 2\rho_2)\phi(r_2) \right] \times \left[\frac{8}{3}(\rho_1^2 - 2\rho_1)\phi(r_1) + 2(\rho_2^2 - 2\rho_2)\phi(r_2) \right],$$

Where $\rho_1 = r_1/b$ and $\rho_2 = r_2/b$.

$$F_{11}^{VIB} = \frac{k_B T}{4} \left(G_2 - \frac{G_1^2}{6} \right); \quad F_{12}^{VIB} = \frac{k_B T}{4} \left(G_{1,1} - \frac{G_1^2}{6} \right); \quad F_{44}^{VIB} = \frac{k_B T}{4} G_{1,1};$$

$$F_{111}^{VIB} = \frac{k_B T}{4} \left(G_3 - \frac{1}{2} G_1 G_2 + \frac{G_1^3}{18} \right); \quad F_{112}^{VIB} = \frac{k_B T}{4} \left(G_{2,1} - \frac{1}{3} G_{1,1} G_1 - \frac{1}{6} G_2 G_1 + \frac{G_1^3}{18} \right);$$

$$F_{123}^{VIB} = \frac{k_B T}{4} \left(G_{1,1,1} - \frac{1}{2} G_1 G_{1,1} + \frac{G_1^3}{18} \right); \quad F_{144}^{VIB} = \frac{k_B T}{4} \left(G_{1,1,1} - \frac{1}{2} G_1 G_{1,1} \right);$$

$$F_{166}^{VIB} = \frac{k_B T}{4} \left(G_{1,1,1} - \frac{1}{2} G_1 G_{1,1} \right); \quad F_{456} = \frac{k_B T}{4} G_{1,1,1}.$$

$$G_1 = \left[\frac{8}{9}(2\rho_1 + 2\rho_1^2 - \rho_1^3)\phi(r_1) + \frac{1}{2}(2\rho_2 + 2\rho_2^2 - \rho_2^3)\phi(r_2) \right] Z,$$

$$G_2 = \left[\frac{8}{27}(-6\rho_1 - 6\rho_1^2 - \rho_1^3 + \rho_1^4)\phi(r_1) + \frac{1}{2}(-6\rho_2 - 6\rho_2^2 - \rho_2^3 + \rho_2^4)\phi(r_2) \right] Z,$$

$$G_3 = \left[\frac{8}{81}(30\rho_1 + 30\rho_1^2 + 9\rho_1^3 - \rho_1^4 - \rho_1^5)\phi(r_1) + \frac{1}{2}(30\rho_2 + 30\rho_2^2 + 9\rho_2^3 - \rho_2^4 - \rho_2^5)\phi(r_2) \right] Z,$$

$$G_{1,1} = \left[\frac{8}{27}(-6\rho_1 - 6\rho_1^2 - \rho_1^3 + \rho_1^4)\phi(r_1) \right] Z,$$

$$G_{2,1} = G_{1,1,1} = \left[\frac{8}{81}(30\rho_1 + 30\rho_1^2 + 9\rho_1^3 - \rho_1^4 - \rho_1^5)\phi(r_1) \right] Z.$$

$$Z = \left[\frac{4}{9}(\rho_1^2 - 2\rho_1)\phi(r_1) + \frac{1}{4}(\rho_2^2 - 2\rho_2)\phi(r_2) \right].$$

Applying Voigt-Reuss-Hill approximation to compute mechanical properties using the SOECs, the expressions for mechanical properties are given below [26]

$$\left\{ \begin{array}{l} B_V = B_R = \frac{C_{11} + 2C_{12}}{3}; \quad B = \frac{B_V + B_R}{2}; \quad p = \frac{B}{G}; \quad Y = \frac{9GB}{G + 3B}; \quad G_V = \frac{C_{11} - C_{12} + 3C_{44}}{5}; \\ G_R = \frac{5[(C_{11} - C_{12})C_{44}]}{4[C_{44} + 3(C_{11} - C_{12})]}; \quad G = \frac{G_V + G_R}{2}; \quad H = 2 \left(\frac{G}{p^2} \right)^{0.585}; \\ \sigma = \frac{3B - 2G}{6B + 2G}; \quad Z_A = \frac{2C_{44}}{C_{11} - C_{12}}; \end{array} \right. \quad (3)$$

where B = bulk modulus; G = shear modulus; H = Vicker's hardness; σ = Poisson's ratio; Z_A = Zener anisotropic parameter; sub script V and R stand for Voigt's and Reuss average methods of approximations for the upper and lower bounds on strain and stress. These parameters provide information about the Born's stability, microhardness, nature and strength of ScN.

The ultrasonic velocities have been calculated with the help of second order elastic constants (C_{11}, C_{12}, C_{44}) and density (ρ) of the material. When ultrasonic wave passes through the ScN, it gets diffused into three modes of transmission. These three modes are comprised of one longitudinal mode (V_L) and two shear modes (V_{S1}, V_{S2}). The expressions for ultrasonic velocities (V_L, V_{S1} and V_{S2}) for the ScN are given below [26]:

$$\left\{ \begin{array}{l} \text{Along } \langle 100 \rangle \text{ direction: } V_L = \sqrt{\frac{C_{11}}{\rho}}, \quad V_{S1} = V_{S2} = \sqrt{\frac{C_{44}}{\rho}} \\ \text{Along } \langle 110 \rangle \text{ direction: } V_L = \sqrt{\frac{C_{11} + C_{12} + 2C_{44}}{2\rho}}, \quad V_{S1} = \sqrt{\frac{C_{44}}{2\rho}}, \quad V_{S2} = \sqrt{\frac{C_{11} - C_{12}}{2\rho}} \\ \text{Along } \langle 111 \rangle \text{ direction: } V_L = \sqrt{\frac{C_{11} + 2C_{12} + 2C_{44}}{2\rho}}, \quad V_{S1} = V_{S2} = \sqrt{\frac{C_{11} - C_{12} + C_{44}}{2\rho}} \end{array} \right\}, \quad (4)$$

where C_{11}, C_{12}, C_{44} are the second order elastic constants and ρ is density, V_L is longitudinal ultrasonic velocity, V_{S1} and V_{S2} are two shear ultrasonic velocities.

The Debye average velocity (V_D) is a valuable parameter to define the thermo-physical behaviour of the ScN. The direction-oriented V_D along the different modes can be defined as [26]:

$$V_D = \left[\frac{1}{3} \left(\frac{1}{V_L^3} + \frac{1}{V_{S1}^3} + \frac{1}{V_{S2}^3} \right) \right]^{-1/3}. \quad (5)$$

Thermal conduction in ScN is affiliated with the diffusion of energy via different degrees of freedom. The expression for the Debye temperature [27] is given below:

$$\theta_D = \frac{h}{k_B} \left(\frac{3nN\rho}{4\pi M} \right)^{1/3} V_D. \quad (6)$$

where M = molecular weight, ρ = density, h = Planck's constant, N = Avogadro's number, k_B = Boltzmann constant, n = number of the atoms per unit cell and V_D = Debye average velocity.

Thermal conductivity (κ) is a function of crystalline phase, Debye temperature and the doping phase of ScN. The thermal conductivity is verbalized as [28]

$$\kappa = \frac{\overline{AM} \delta \theta_D^3 n^{1/3}}{\gamma^2 T} \quad (7)$$

where T = temperature, \overline{M} = molecular weight in amu, δ (in Å) = the cube root of volume per atom and n = number of atoms per unit cell and γ^2 = average square of Grüneisen parameter.

The ultrasonic attenuation occurs due to the phonon-phonon interaction process and due to thermoelastic relaxation mechanism at higher temperature ($\cong 300$ K). Akhiezer [29] proposed the phonon viscosity mechanism, which was upgraded by Bömmel and Dransfeld [30]. The final version of the theory was given by Mason [31]. The expressions to evaluate Akheiser loss are given below [32]:

$$\left(\frac{\alpha}{v^2} \right) = \frac{4\pi^2 \tau E_0 D}{6\rho V^3}. \quad (8)$$

where α = ultrasonic attenuation coefficient, E_0 = energy density and v = the frequency of acoustic wave, D = the coupling constant. The evaluation of E_0 has been done by (θ_D/T) tables of

AIP Handbook [33]. The thermal relaxation time (τ_{th}) signifies the time in which thermal phonons may regain its original position by the change of the ultrasonic energy into the thermal energy on the application of ultrasonic waves. The expression to compute the relaxation time [32] is given as

$$\tau_{th} = \tau_s = \frac{\tau_L}{2} = \frac{3\kappa}{C_V V_D^2} \quad (9)$$

it is extremely clear that the thermal relaxation time is directly proportional to the thermal conductivity and in turn ultrasonic attenuation is directly proportional to the thermal relaxation time. C_V is the specific heat per unit volume and can be figured out by (θ_D/T) tables of AIP Handbook [33]. The acoustic coupling constant (D) for the ScN is given by [32]

$$D = 9 \langle (\gamma_i^j)^2 \rangle - \frac{3 \langle \gamma_i^j \rangle^2 C_V T}{E_0} \quad (10)$$

where γ_i^j is ultrasonic Grüneisen parameter which can be evaluated by applying the values of SOECs and TOECs.

When an ultrasonic wave passes through a crystal, there is transmission of the thermal energy from the compressed region to the expanded region associated with the wave. The thermal relaxation process causes the thermo-elastic loss between the two regions of the wave. The expression for the thermo-elastic loss is given as [32]

$$\left(\frac{\alpha}{v^2}\right)_{th} = \frac{4\pi^2 \langle \gamma_i^j \rangle^2 \kappa T}{2\rho V_L^5} \quad (11)$$

where ρ is the density of ScN, V_L is the longitudinal wave velocity, κ is thermal conductivity, T is temperature and $\langle \gamma_i^j \rangle$ is average Grüneisen parameter.

3. RESULTS AND DISCUSSION

The second- and third-order elastic constants (SOECs and TOECs) have been figured out for the B1 and B2 structured scandium nitride using two basic parameters i.e., nearest neighbor distance (r_0) and hardness parameter (b). The values for r_0 [8] and b [34] for the ScN are given as B1 phase -- $r_0 = 4.57 \text{ \AA}$; $b = 0.295 \text{ \AA}$; B2 phase -- $r_0 = 2.87 \text{ \AA}$; $b = 0.303 \text{ \AA}$.

The evaluated SOECs and TOECs for ScN at 300 K are presented in Table 1.

Table 1. SOECs and TOECs (in GPa) for ScN at 300 K.

Phase	C_{11}	C_{12}	C_{44}	C_{111}	C_{112}	C_{123}	C_{144}	C_{166}	C_{456}
B1 phase	349.60	33.91	37.32	-2912	-140.5	45.19	58.15	-168.56	57.4
	331.00 ^[8]	96.00 ^[8]	163.85 ^[8]						
	380.9 ^[35]	104.56 ^[35]	167.18 ^[35]						
B2	200.05	72.96	61.18	-2174.1	-71.14	43.89	46.32	-82.27	34.101

phase	571.61 ^[8]	53.05 ^[8]	101.6 ^[8]						
-------	-----------------------	----------------------	----------------------	--	--	--	--	--	--

It is depicted from Table 1 that the B1 phase of ScN shows greater values of C_{11} , C_{123} , C_{144} compared to the B2 phase, while the values of C_{12} and C_{44} are greater than those in the B1 phase. The calculated values indicated that C_{11} is greater in the B1 phase while C_{44} is greater in the B2 phase for ScN. Table 1 reveals that the values of the SOECs deviate from 5 % to 77 % from the available literature [8, 35]. It happened due to different types of SOECs computing models such as full-potential linearized augmented plane wave method (FP-LAPW) and density functional theory (DFT). The enumerated values of SOECs follow the Born stability criteria ($C_{11} + 2C_{12} > 0$, $C_{44} > 0$, $C_{11} - C_{12} > 0$ and $C_{11} > B > C_{12}$), which predicts the elastic stability of ScN at room temperature in both phases. This type of nature of the ScN resembles with the B1 structured semi metallic [36] and intermetallics [37]. The Cauchy pressure (C_p) has been defined by ($C_{12} - C_{44}$) and is used to describe the structure of atomic bonding in the ScN. On the account of value of C_p , scandium nitride shows a metallic bearing in both chosen phases as depicted from Table 1. Thus, the presented theoretical approach to evaluate the SOECs and TOECs is well justified with the other reported values [36,37].

The mechanical constants such as bulk modulus (B), shear modulus (G), Young's modulus (Y), Poisson's ratio (σ), Zener anisotropic factor (Z_A) and Vicker's hardness (H) have been evaluated using Eq. (3). The figured values of B , Y , G , Z_A , σ and H are presented in Table 2 with density of the ScN and Pugh's indicator (B/G).

Table 2. B (GPa), G (GPa), Y (GPa), B/G ratio, Z_A , ρ (g/cm³), H (GPa) and σ of scandium nitride at 300 K.

Parameter	B	Y	G	B/G	Z_A	ρ	σ	H
B1 Phase	139.14	179.02	69.63	1.9	0.23	4.1	0.28	10.26
	174.70 ^[8]	338.12 ^[8]	143.57 ^[8]	-	0.13 ^[8]	4.12 ^[8]	0.18 ^[8]	24.7 ^[8]
	201.12 ^[13]							
	196.67 ^[35]							
B2 Phase	114.18	174.12	69.08	1.6	0.96	2.05	0.24	21.53
	155.17 ^[8]	205.93 ^[8]	-76.13 ^[8]	-	0.79 ^[8]	4.35 ^[8]	0.79 ^[8]	-
	183.67 ^[13]							

The shear modulus represents the material's hardness whereas the Young's modulus provides its stiffness. A solid with a high Young's modulus is inelastic or stiff, here the obtained results show that Young's modulus of the ScN in B1 phase is slightly greater than the B2 phase and the shear modulus in the B2 phase is greater than that in the B1 phase. It is due to the higher stiffness (C_{11}) value in the B1 phase and higher shear hardness (C_{44}) value in the B2 phase for ScN. The bulk modulus (B) can be beneficial for the measurement of resistance to volume change due to pressure applied on it. It may be predicted from Table 2 that the values of mechanical constants vary from 9 % to 60 % compared to the existing values of mechanical constants of the ScN in the literature [8,13,35]. Thus it is obvious that the chosen potential model is not relevant to calculating the elastic moduli in the complex case of scandium nitride as can be seen from the comparison with the experimental data for the B1 phase of ScN and with the calculations on the basis of advanced approaches. From Table 2, the calculated bulk modulus for

the ScN in B1 phase is higher, therefore the B1 phase has the strongest opposition to any change in volume. On the other hand, the ScN in B1 phase has a slightly higher shear modulus as compared to that in the B2 phase which determines the material's resistance to reversible deformation under shear force.

The material's hardness can be attained with the Vickers hardness (H) parameter. In coating applications, materials with higher hardness are required and in the present investigation H is estimated to be 10.26 GPa and 21.53 GPa in the B1 and B2 phases, respectively. It can be predicted from Table 2 that the ScN in B2 type structure is harder than in the B1 phase. According to Pugh [38] and Frantsevich *et al.* [39], if the Pugh's indicator B/G is greater than 1.75 the chosen substance is ductile otherwise brittle. The estimated values in Table 2 reveal that the ScN is ductile in B1 phase whereas brittle in the B2 phase. The Zener's anisotropic factor (Z_A) gives an indication regarding the degree of anisotropy in a material and is equal to one for an isotropic crystal. The computed values of Z_A are equal to 0.23 for the B1 phase and 0.96 for the B2 phase, which are not exactly equal to 1, thus the ScN is an elastically anisotropic material in both phases in the present study. Comparison of the mechanical parameters of the ScN with other similar the B1 and B2 structured compounds such as boron mononitrides [26] and the B2 structured intermetallics [37,40], provides justification for our methodology.

The acoustic wave velocities and Debye average velocities have been evaluated with Eqs. (4) and (5). The Debye temperature (θ_D) and the relaxation time (τ) have been estimated with Eq. (6) and Eq. (9), respectively. The evaluated values of ultrasonic velocities (V_L, V_{S1}, V_{S2}, V_D), Debye temperature (θ_D) and the relaxation time (τ) are represented in Table 3 along $\langle 100 \rangle$, $\langle 110 \rangle$ and $\langle 111 \rangle$ orientations.

Table 3. Orientation-dependent values of V_L, V_{S1}, V_{S2}, V_D (in 10^3 ms^{-1}), θ_D (in K) and τ (in ps) of ScN at 300 K.

Direction→ Parameter↓	$\langle 100 \rangle$		$\langle 110 \rangle$		$\langle 111 \rangle$	
	B1	B2	B1	B2	B1	B2
V_L	9.23	4.78	7.47	4.75	6.78	4.79
V_{S1}	3.01	2.64	3.02	2.65	5.35	2.68
V_{S2}	3.01	2.64	6.20	2.69	5.35	2.68
V_D	3.38	2.91	4.06	2.94	5.62	2.96
θ_D	547	480	656	484	908	485
τ	3.55	2.45	5.24	3.41	5.65	3.87

Table 3 indicates that the calculated velocities along the shear mode of the ScN are smaller than those along the longitudinal mode for the B1 phase and B2 phase at 300 K. The Debye average velocities and Debye temperature along the $\langle 100 \rangle$, $\langle 110 \rangle$ and $\langle 111 \rangle$ crystallographic directions of the ScN are shown in Figure 1 and Figure 2, respectively.

Figures 1 and 2 show that the Debye mean velocities and the Debye temperatures of ScN are highest along $\langle 111 \rangle$ direction in both phases. The Debye mean velocities are the average of ultrasonic longitudinal and shear velocities which are highest along the $\langle 111 \rangle$ direction. The Debye temperature of the ScN directly depends on Debye velocity, that's why it is highest along

the $\langle 111 \rangle$ direction. The Debye temperatures are higher for the B1 phase than those for the B2 phase at room temperature along the $\langle 100 \rangle$, $\langle 110 \rangle$ and $\langle 111 \rangle$ directions. Thus, the ScN in B1 phase has better thermal performance than in the B2 phase.

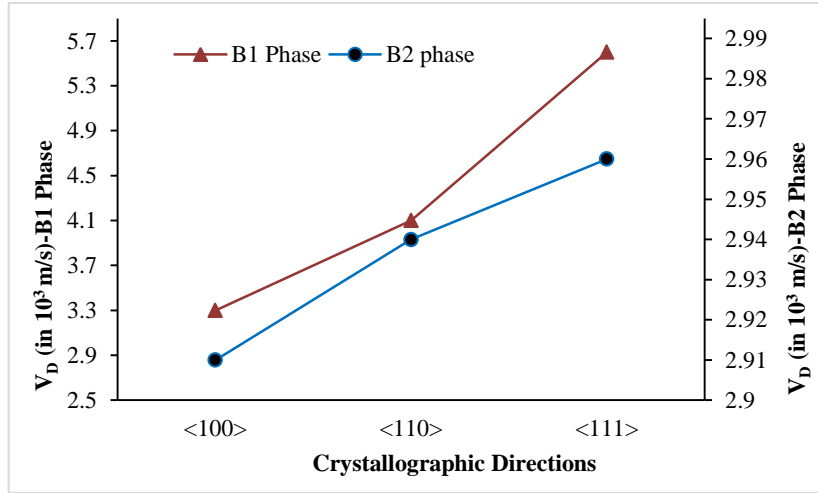


Figure 1. Direction-dependent Debye velocity (V_D) of ScN in B1 and B2 phases.

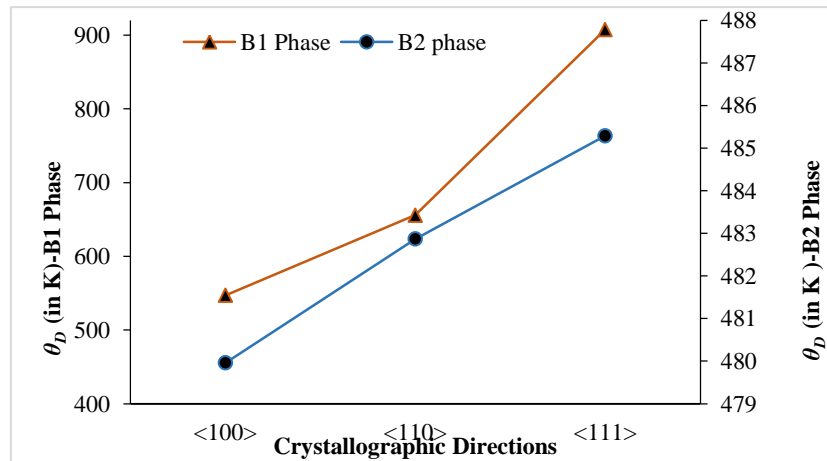


Figure 2. Direction-dependent Debye temperature (θ_D) of ScN in B1 and B2 phases.

The thermal relaxation time is directly proportional to thermal conductivity as given in Eq. (9). It is obvious from Table 3 that the relaxation time due to thermal mechanism is of the order of picosecond for the ScN, which confirms the intermetallic nature of the ScN [41]. The ultrasonic Grüneisen parameter (UGPs) $\langle \gamma_i^j \rangle$, $\langle \gamma_i^j \rangle^2$, $\langle (\gamma_i^j)^2 \rangle$ were calculated by means of the SOECs and TOECs along different crystallographic directions. Then, acoustic coupling constants (D_L , D_{S1} , D_{S2}) were enumerated with the use of the UGPs according to Eq. (10), the specific heat capacity, the Debye temperature and energy density values. Finally, ultrasonic attenuation $\left(\frac{\alpha}{v^2}\right)_{th}$, $\left(\frac{\alpha}{v^2}\right)_L$, $\left(\frac{\alpha}{v^2}\right)_{S1}$, $\left(\frac{\alpha}{v^2}\right)_{S2}$, $\left(\frac{\alpha}{v^2}\right)_{total}$ for ScN have been computed with the help of Eq. (8) and Eq. (11) along the $\langle 100 \rangle$, $\langle 110 \rangle$ and $\langle 111 \rangle$ crystallographic orientations at

300 K. The acquired values of the UGPs, acoustic coupling constants and ultrasonic attenuation are presented in Table 4.

Table 4. $\langle \gamma_i^j \rangle$, $\langle \gamma_i^j \rangle^2$, $\langle (\gamma_i^j)^2 \rangle$, κ (in $\text{Wm}^{-1}\text{K}^{-1}$), D_L, D_{S1}, D_{S2} , $\left(\frac{\alpha}{v^2}\right)_{th}$, $\left(\frac{\alpha}{v^2}\right)_L$, $\left(\frac{\alpha}{v^2}\right)_{S1}$, $\left(\frac{\alpha}{v^2}\right)_{S2}$, $\left(\frac{\alpha}{v^2}\right)_{total}$ (all $\left(\frac{\alpha}{v^2}\right)$ are in $10^{-16} \text{Nps}^2\text{m}^{-1}$) of ScN at 300 K along $\langle 100 \rangle$, $\langle 110 \rangle$ and $\langle 111 \rangle$ orientations.

Direction	$\rightarrow \langle 100 \rangle$		$\langle 110 \rangle$		$\langle 111 \rangle$	
Parameter	B1	B2	B1	B2	B1	B2
$\langle \gamma_i^j \rangle$	0.08	0.099	-0.17	-0.38	-0.13	-0.21
$\langle \gamma_i^j \rangle^2$	0.01	0.0099	0.034	0.15	0.016	0.05
$\langle (\gamma_i^j)^2 \rangle$	0.59	0.721	1.70	1.89	0.34	0.66
κ	20.25	18.34	20.01	16.04	34.36	23.05
D_L	5.311	6.44	15.11	16.26	2.93	5.73
D_{S1}	1.19	8.89	0.26	0.21	1.18	1.77
D_{S2}	1.19	8.89	14.57	14.15	1.18	1.77
$\left(\frac{\alpha}{v^2}\right)_{th}$	0.02	0.02	0.04	0.16	0.04	0.03
$\left(\frac{\alpha}{v^2}\right)_L$	0.38	1.80	1.29	4.50	0.25	2.54
$\left(\frac{\alpha}{v^2}\right)_{S1}$	1.23	7.79	0.17	0.17	1.03	2.06
$\left(\frac{\alpha}{v^2}\right)_{S2}$	1.23	7.79	1.08	10.74	1.03	2.06
$\left(\frac{\alpha}{v^2}\right)_{total}$	2.84	17.41	2.57	15.56	2.32	6.71

Table 4 reveals that the thermal conductivity of the ScN is highest in the B1 phase along the $\langle 111 \rangle$ direction at 300 K. The thermal conductivity of the ScN is directly proportional to the cube of the Debye temperature and inversely proportional to the square of Grüneisen parameter. The thermal conductivity of the ScN in B1 phase along the $\langle 111 \rangle$ direction is the highest because of the highest value of Debye temperature and lesser value of Grüneisen parameter. Table 4 also shows that the ultrasonic attenuation in the ScN due to thermo-elastic relaxation mechanism $\left(\frac{\alpha}{v^2}\right)_{th}$ is very small in comparison with Akheiser damping (phonon-phonon interaction mechanism) in both phases. Thus, the dominant cause of the non-linear attenuation is the phonon-phonon interaction mechanism at 300 K in the case of scandium nitride. The total ultrasonic attenuation $\left(\frac{\alpha}{v^2}\right)_{total} = \left(\frac{\alpha}{v^2}\right)_{th} + \left(\frac{\alpha}{v^2}\right)_L + \left(\frac{\alpha}{v^2}\right)_{S1} + \left(\frac{\alpha}{v^2}\right)_{S2}$ is shown in Figure 3 for showing the comparison between the B1 (NaCl-type) and B2 (CsCl-type) phases of the ScN.

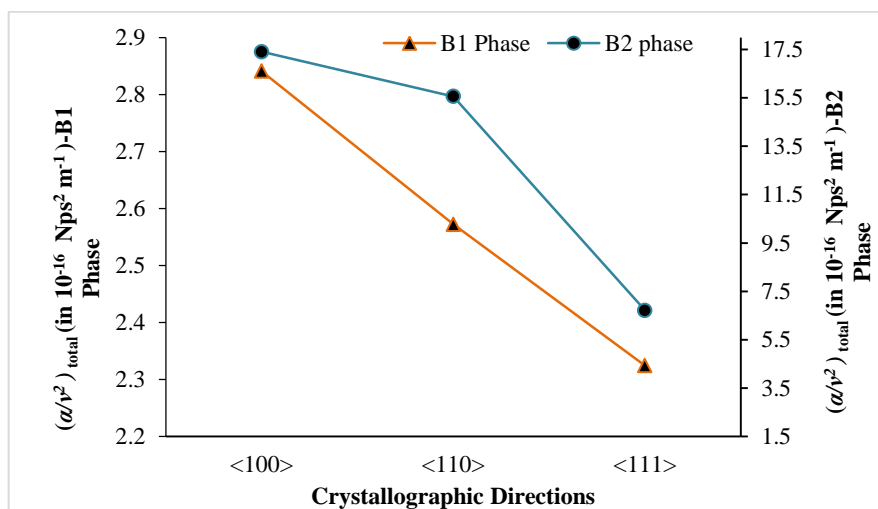


Figure 3. Direction-dependent total ultrasonic attenuation of ScN (in $10^{-16} \text{ Nps}^2 \text{ m}^{-1}$) in both B1 and B2 phases.

It is a very important fact that the ultrasonic attenuation depends upon the nature of the material and modes of wave propagation. The favourable orientation for wave transmission is along <111> because the least ultrasonic attenuation has been found in this direction. From Figure 3, it is also depicted that scandium nitride offers smaller ultrasonic attenuation in the B1 phase while larger in the B2 phase. It is known that ultrasonic attenuation directly depends upon the acoustic coupling constant and ultrasonic Grüneisen parameter while inversely to the acoustic velocity of the ScN. The behaviour of non-destructive ultrasonic attenuation for the ScN is comparable to previous studies on boron mononitrides [26], platinum group metal carbides [28], alkali halides [32], and intermetallics [37, 40].

4. CONCLUSIONS

The interaction potential approach is utilized to figure out the second- and third-order elastic stiffness constants in B1 and B2 phases of scandium nitride at 300 K and is validated with existing results. The ScN is elastically and mechanically stable in both B1 (NaCl-type) and B2 (CsCl-type) phases. The ScN with NaCl-B1 structure is stiffer compared to CsCl-B2 phase. The Poisson's ratio and Pugh's ratios reveal that the ScN has ductile nature in the B1 phase whereas brittle in the B2 phase. For B1 phase, $Z_A = 0.23$ and for B2 phase, $Z_A = 0.96$ which are not exactly equal to one, hence the B1 and B2 phases of ScN show an isotropic nature. The higher values of Debye temperatures and thermal conductivities in the B1 phase of ScN show better thermophysical activity in the B1 phase. The thermal relaxation times for the B1 and B2 phases are of the picosecond order, which confirms the intermetallic character of the B1 and B2 phases of ScN. The attenuation of ultrasonic waves due to thermo-elastic interaction mechanism $\left(\frac{\alpha}{v^2}\right)_{th}$ is very little in contrast to the Akhiezer loss. Thus, the phonon-phonon interaction is a controlling factor in both phases at 300 K. The total ultrasonic attenuation in the B1 phase of ScN is lower than in the B2 phase. So the B1 phase of ScN is more applicable than its B2 phase. The Debye mean velocity, Debye temperature and thermal conductivity are the highest and the ultrasonic attenuation is the lowest along the <111> direction, which indicates that the <111> direction is most suitable for industrial purposes. The obtained results provide a better

knowledge of thermo-physical, mechanical and non-destructive ultrasonic characteristics in both B1 and B2 phases of ScN.

Credit authorship contribution statement. ANURAG SINGH: Investigation, Methodology, Manuscript Drafting. JYOTI BALA: Formal analysis, Manuscript Drafting. SHAKTI PRATAP SINGH: Formal analysis, Discussion. DEVRAJ SINGH: Supervision, Analysis and Discussion.

Declaration of competing interest. The authors declare that they have no known competing financial interests or personal relationships that could have appeared to influence the work reported in this paper.

REFERENCES

1. Zheng F., Xiao, J. Xie, L. Zhou, Y. Li and H. Dong - Structures, properties and applications of two-dimensional metal nitrides: from nitride MXene to other metal nitrides, *2D Mater.* **9** (2022) 022001. <https://doi.org/10.1088/2053-1583/ac52b3>
2. Biswas B., Saha B. - Development of semiconducting ScN, *Phys. Rev. Materials* **3** (2019) 020301. <https://doi.org/10.1103/PhysRevMaterials.3.020301>
3. Roccaforte, P. Fiorenza, G. Greco, R. L. Nigro, F. Giannazzo, F. Iucolano, M. Saggio - Emerging trends in wide band gap semiconductors (SiC and GaN) technology for power devices, *Microelec. Eng.* **188** (2018) 66. <https://doi.org/10.1016/J.MEE.2017.11.021>
4. Brithen A., Hamad A., Arthur, G. Daniel - Surface and bulk electronic structure of ScN investigated by scanning tunneling microscopy/spectroscopy and optical absorption spectroscopy, *Phys. Rev. B.* **70** (2004) 045303. <https://doi.org/10.1103/PhysRevB.70.045303>
5. Gu Z., Edgar J. H., Pomeroy J., Kuball M., Coffey D. W. - Crystal growth and properties of scandium nitride, *J. Mater. Sci. Mater. Electron.* **15** (2004) 555. <https://doi.org/10.1023/B:JMSE.0000032591.54107.2c>
6. Edgar J. H., Bohnen T., Hageman P. R. - HVPE of scandium nitride on 6H-SiC (0001), *J. Crys. Growth.* **310** (2008) 1075. <https://doi.org/10.1016/J.JCRYSGRO.2007.12.053>
7. Westgren A. - Crystal structure and atomic properties of alloys containing transition elements, *J. Frank. Inst. Eng. Appl. Math.* **577** (1931). [https://doi.org/10.1016/S0016-0032\(31\)90003-3](https://doi.org/10.1016/S0016-0032(31)90003-3)
8. Mnisi B. O. - Density functional theory study of electronic and optical properties of ScN nitride in NaCl-B1, CsCl-B2, ZB-B₃ and NiAs-B₈ phases, *Bull. Mater. Sci.* **45** (1) (2022). <http://dx.doi.org/10.1007/s12034-021-02601-4>
9. Takeuchi N. - First-principles calculations of the ground-state properties and stability of ScN, *Phys. Rev. B.* **65** (2002) 045204. <https://doi.org/10.1103/PhysRevB.65.045204>
10. Duman S., Bağcı S., Tütüncü H. M., Uğur G., Srivastava G. P. - Theoretical study of the structural, electronic and dynamical properties of rocksalt ScN and GaN, *Dia. Rel. Mat.* **15** (2006) 1175. <https://doi.org/10.1016/j.diamond.2005.12.003>
11. Maachou A., Amrani B., Driz M. - Structural and electronic properties of III-V scandium compounds, *Phys. B. Cond. Mat.* **388** (2007) 384. <https://doi.org/10.1016/j.physb.2006.06.145>
12. Stampfl C., Mannstadt W., Asahi R. - Electronic structure and physical properties of early transition metal mononitrides: Density-functional theory LDA, GGA and screened-exchange LDA FLAPW calculations, *Phys. Rev. B.* **63** (2001) 155106. <https://doi.org/10.1103/PhysRevB.63.155106>

13. Yagoub R., Djabri H. R., Daoud S., Beloufa N., Belarbi M., Haichour A., Zegadi C., Louhibi S., Fasla S. - First principles study of High-pressure phases of ScN, Ukrainian J. Phys. **66** (8) (2021) 699-707. <https://doi.org/10.15407/ujpe66.8.699>
14. Tahri S., Qteish A., Qasir I. I. A., Noureddin M. - Vibrational and thermal properties of ScN and YN: quasi harmonic approximation calculations and anharmonic effects. J. Phys: Condens Matter. **24** (3), 035401 (2012). <https://doi.org/10.1088/0953-8984/24/3/035401>
15. Ambacher O., Mihalic S., Yassine M., Yassine A., Afshar N., Christian B. - Review: Structural, elastic, and thermodynamic properties of cubic and hexagonal Sc_xAl_{1-x}N crystals, J. Appl. Phys. **134** (2023) 160702. <https://doi.org/10.1063/5.0170742>
16. Seksaria H., Kaur A., Singh K., Sarkar A. D.-Hexagonal and tetragonal ScX (X = P, As, Sb) nanosheets for optoelectronics and straintronics, Appl. Surf. Sci. **615** (2023) 156306. <https://doi.org/10.1016/j.apsusc.2022.156306>
17. Xue W., Yu Y., Zhao Y., Han H. L., Gao T. - First principles calculations of the electronic, dynamical, and thermodynamic properties of the rock salt ScX (X = N, P, As, Sb), Comput. Mater. Sci. **45** (2009) 1025. <https://doi.org/10.1016/j.commatsci.2009.01.007>
18. Sukkabet W. - Structural and magnetic properties of transition-metal doped scandium nitride (ScN): spin density functional theory, J. Phys. B: Cond. Mat. **570** (2019) 236. <https://doi.org/10.1016/j.physb.2019.06.04>
19. Ekuma C. E., Bagayoko D., Jarrell M., Moreno J. - Electronic, structural, and elastic properties of metal nitrides XN (X = Sc, Y): A first principle study, A. I. P. Adv. **2** (2012) 032163. <https://doi.org/10.1063/1.4751260>
20. Born M., Mayer J. E. - Zur Gittertheorie der Ionenkristalle, Z. Phys. **75** (1) (1932). <https://doi.org/10.1007/BF01340511>
21. Brugger K. - Thermodynamic definition of higher order elastic coefficients, Phys. Rev. **133** (1964) A1611. <https://doi.org/10.1103/PhysRev.133.A1611>
22. Leibfried G., Haln H. - Zur Temperaturabhängigkeit der elastischen Konstanten von Alkalihalogenidkristallen, Zeitschrift für Phys. **150** (1958) 497. <https://doi.org/10.1007/BF01418637>
23. Leibfried G., Ludwig W. - Theory of anharmonic effects in crystals, Solid stat. Phys. **12** (1961) 275. [https://doi.org/10.1016/S0081-1947\(08\)60656-6](https://doi.org/10.1016/S0081-1947(08)60656-6)
24. Ghate P. B. - Third order elastic constants of alkali halide crystals, Phys. Rev. A **139** (1965) 1666. <https://doi.org/10.1103/PhysRev.139.A1666>
25. Mori S., Hiki Y. - Calculation of the third- and fourth-order elastic constants of alkali halide crystals, J. Phys. Soc. Jpn. **45** (1978) 1449. <https://doi.org/10.1143/JPSJ.45.1449>
26. Bala J., Singh S. P., Verma A. K., Singh D. K., Singh D. - Elastic, mechanical and ultrasonic studies of boron mononitrides in two different structural phases, Indian J. Phys. **96** (2022) 3191-3200. <https://doi.org/10.1007/s12648-021-02278-9>
27. Jyoti B., Singh S. P., Gupta M., Tripathi S., Verma A. K., Singh D., Yadav R. R.- Ultrasonic and thermophysical properties of cobalt nanowires, Acoust. Phys. **97**, 584-589 (2021). <https://doi.org/10.1134/S1063771021330022>
28. Singh A., Singh D. - Influence of temperature and orientation on elastic, mechanical, thermophysical and ultrasonic properties of platinum group metal carbides, Johnson Matthey Technol. Rev. **68** (1) (2024) 49-59. <https://doi.org/10.1595/205651323x16902884637568>.

29. Akhiezer A. - On the absorption of sound in solids, *J. Phys. (Moscow)* **1** (1939) 277-287.
30. Bömmel H. E., Dransfeld K. - Excitation and attenuation of hypersonic waves in quartz, *Phys. Rev.* **117** (1960) 1245-1252. <https://doi.org/10.1103/PhysRev.117.1245>
31. Mason W. P. - Effect of impurities phonons process on the ultrasonic attenuation of germanium crystal quartz and silicon, In W. P. Mason (Ed.) *Physical Acoustics: Principle and methods*, Vol. III B, Academic press, New York, 1965, pp. 277. <https://doi.org/10.1016/B978-0-12-395669-9-50013-8>.
32. Singh A., Singh D. - Investigation of alkali halide crystals AX (A = Li, Na, K and X = F, Cl, Br) by elastic, mechanical and ultrasonic analysis, *Z. Naturforsch. A.* **78** (10) (2023) 947-958. <https://doi.org/10.1515/zna-2023-0138>.
33. Gray D. E. - *American Institute of Physics Handbook*, Third Ed., Mc Graw-Hill, New York, 1972.
34. Tosi M. P. - Cohesion of ionic solids in the Born model, In: F. Seitz and D. Turnbull (Eds.), *Solid State Physics*, Vol. **16**, Academic Press, New York, 1964, pp. 1-120. [https://doi.org/10.1016/s0081-1947\(08\)60515-9](https://doi.org/10.1016/s0081-1947(08)60515-9).
35. Feng W., Cui S., Hu H., Zhang G., Gong Z. L. Z. - Phase stability, electronic and elastic properties of ScN, *Phys. B.* **405** (2010) 2599-2603. <https://doi.org/10.1016/j.physb.2010.03.042>
36. Singh D., Tripathi S., Pandey D. K., Gupta A. K., Singh D. K., Kumar J. - Ultrasonic wave propagation in semimetallic single crystals, *Mod. Phys. Lett. B.* **25** (2011) 2377. <https://doi.org/10.1142/S0217984911027686>
37. Yadav C. P., Pandey D. K., Singh D. - Elastic and ultrasonic studies on RM (R = Tb, Dy, Ho, Er, Tm; M = Zn, Cu) compounds. *Z. Naturforsch. A.* **74** (2019) 1123. <https://doi.org/10.1515/zna-2019-0041>
38. Pugh S. F. - XCII Relations between the elastic moduli and the plastic properties of polycrystalline pure metals, *Philos. Mag. J. Sci.* **45** (1954) 823. <https://doi.org/10.1080/14786440808520496>
39. Frantsevich I. N., Voronov F. F., Bokuta S. A. - *Hand book on Elastic Constants and Elastic Moduli of Metals and Insulators*, NaukovaDumka, Kiev, 1982, pp. 60. <https://doi.org/10.1023/B.JMSE.0000032591.54107.2c>
40. Bala J., Singh D., Pandey D. K., Yadav C. P. - Mechanical and thermophysical properties of ScM (M: Ru,Rh,Pd,Ag) intermetallics, *Int. J. Thermophys.* **41** (2020) 46. <http://dx.doi.org/10.1007/s10765-020-02624-9>
41. Singh D., Pandey D. K., Yadawa P. K. - Ultrasonic wave propagation in rare-earth monochalcogenides, *Cent. Eur. J. Phys.* **7** (2009) 198. <https://doi.org/10.2478/s11534-008-0130-1>